Supporting Information

Prediction of strong solvatochromism in a molecular photocatalyst

Miftahussurur Hamidi Putra,† Benedikt Bagemihl,‡ Sven Rau,‡ and Axel Groß*,†,¶

†Institute of Theoretical Chemistry, Ulm University, 89069 Ulm, Germany

‡Institute of Inorganic Chemistry I, Materials and Catalysis, Ulm University, 89069 Ulm, Germany

¶Helmholtz Institute Ulm (HIU), Electrochemical Energy Storage, 89069 Ulm, Germany

E-mail: Axel.Gross@uni-ulm.de

S1 MPE Solvation Method

The solvation free energy (ΔG_{sol}) determined within the MPE implicit solvation method can be approximated as

$$\begin{aligned}\Delta G_{\mathrm{sol}}(\rho_{\mathrm{iso}},\alpha,\beta) &= \Delta G_{\mathrm{el}}(\rho_{\mathrm{iso}}) + \Delta G_{\mathrm{ne}}(\rho_{\mathrm{iso}},\alpha,\beta)\\ &= \Delta G_{\mathrm{el}}(\rho_{\mathrm{iso}}) + \alpha O(\rho_{\mathrm{iso}}) + \beta V(\rho_{\mathrm{iso}})\end{aligned} \tag{S1}$$

with ρ_{iso} is the isosurface cavity parameter and $\Delta G_{\mathrm{el}}(\rho_{\mathrm{iso}})$ is the electrostatic contribution to the free energy that can be defined as

$$\Delta G_{\mathrm{el}}(\rho_{\mathrm{iso}}) = U_{\mathrm{cont}}(\rho_{\mathrm{iso}}) - U_{\mathrm{vac}} \tag{S2}$$

Table S1: Estimated ρ_{iso} parameter for $RuPtI_2$ in acetonitrile.

Basis Sets	Data Sets	ρ_{iso} (meV/Å^3)	MAE (kcal/mol)
Light	Neutral	5.36	0.72
	Cation	38.00	3.24
Tight	Neutral	6.00	1.04
	Cation	40.00	3.31
Really-Tight	Neutral	6.00	1.03
	Cation	40.00	3.31

where $U_{\text{cont}}(\rho_{\text{iso}})$ is the total energy of the molecule in the implicit solvent derived from DFT calculations and U_{vac} is the total energy in vacuum.[1–4] In addition, the contribution of the non-electrostatic factor is approximated here by linear regression as

$$\Delta G_{\text{ne}}(\rho_{\text{iso}}, \alpha, \beta) = \alpha O(\rho_{\text{iso}}) + \beta V(\rho_{\text{iso}}) \tag{S3}$$

where $O(\rho_{\text{iso}})$ and $V(\rho_{\text{iso}})$ are the quantum surface and volume cavity. The parameters α, β and ρ_{iso} are determined by fitting the solvation free energy to suitable reference data.[1,5] Thus, we have three parameters that are needed to be defined in order to apply the MPE solvation method, α, β and ρ_{iso}.

However, the determination of these three parameters is computationally rather demanding. In order to reduce the computational effort, one can use a test set from Marenich *et al.*[6] consisting of 7 neutral molecules and 39 cationic molecules. Thus one arrives at $\alpha = 46.4$ dyn/cm and $\beta = -0.5$ GPa.[5] The only parameter that is left to be determined is the isosurface cavity parameter ρ_{iso}. We have calculated the mean absolute error (MAE) in the solvation free energy between DFT and and the reference data[1,5] for an equidistant set of the isosurface cavity parameter in the interval $\rho_{\text{iso}} \in [0, 100]$ meV/Å^3. The minimum MAE is then determined from a spline cubic interpolation of the MAE values as a function of ρ_{iso}. We have determined ρ_{iso} for three different basis sets, light, tight, and really tight.

The optimized ρ_{iso} for three different basis sets and two different data sets including its MAE is summarized in Tab. S1. Figure S1 shows the correlation plot between measured

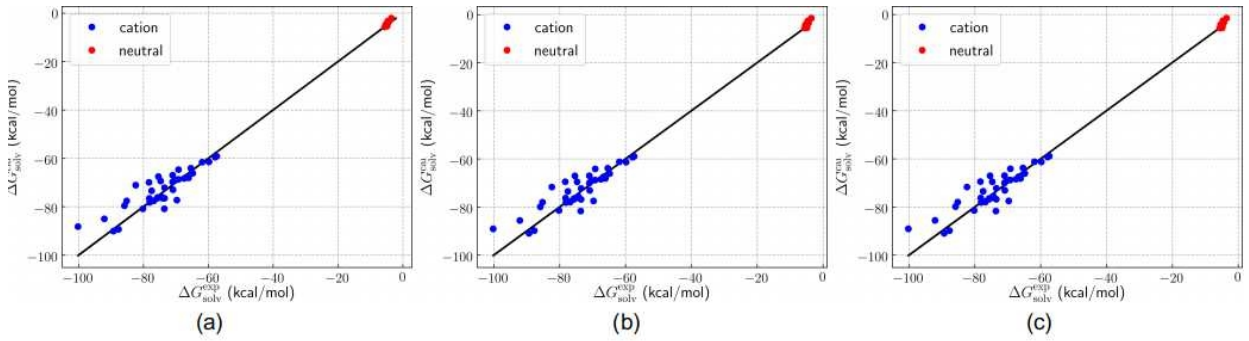

Figure S1: Correlation plot of the solvation free energy in acetonitrile between experimental ($\Delta G^{\text{exp}}_{\text{solv}}$) and calculated ($\Delta G^{\text{calc}}_{\text{solv}}$) results using the FHI-AIMS code with three different basis-sets: (a) light, (b) tight, and (c) really-tight.

Table S2: Comparison of the performance of the MPE method used in this work with other implicit solvent methods [6] for solvated neutral molecules.

Solvent Method	Basis Sets	XC Functional	Software	N	ε	MAE (kcal/mol)
SMD	631G*	mPW1PW	Gaussian 03	7	35.69	0.63
SM8	631G(d)	mPW1PW	Gaussian 03	7	35.69	0.61
IEF-PCM (UA0)	631G(d)	mPW1PW	Gaussian 03	7	35.69	7.21
IEF-PCM (UAHF)	631G(d)	mPW1PW	Gaussian 03	7	35.69	5.14
CPCM	631G(d)	B3LYP	GAMESS	7	35.69	1.35
PB	631G(d)	B3LYP	Jaguar	7	35.69	1.75
GCOSMO	631G(d)	B3LYP	NWCHEM	7	35.69	4.75
MPE	Light	B3LYP	FHI-AIMS	7	35.69	0.73
	Tight	B3LYP	FHI-AIMS	7	35.69	1.05
	Really Tight	B3LYP	FHI-AIMS	7	35.69	1.03

Table S3: Comparison of the performance of the MPE method used in this work with other implicit solvent methods [6] for solvated cationic molecules.

Solvent Method	Basis Sets	XC Functional	Software	N	ε	MAE (kcal/mol)
SMD	6-31G*	M05-2X	Gaussian 03	39	35.69	4.9
SM8	6-31G(d)	mPW1PW	Gaussian 03	39	35.69	7.2
IEF-PCM (UA0)	6-31G(d)	mPW1PW	Gaussian 03	39	35.69	18.7
IEF-PCM (UAHF)	6-31G(d)	mPW1PW	Gaussian 03	39	35.69	24.2
CPCM	6-31G(d)	B3LYP	GAMESS	39	35.69	14.6
PB	6-31G(d)	B3LYP	Jaguar	39	35.69	7.3
GCOSMO	6-31G(d)	B3LYP	NWCHEM	39	35.69	4.6
MPE	Light	B3LYP	FHI-AIMS	39	35.69	3.23
	Tight	B3LYP	FHI-AIMS	39	35.69	3.28
	Really Tight	B3LYP	FHI-AIMS	39	35.69	3.29

and calculated solvation free energies in acetonitrile for a test set. In order to validate our approach, we compare the MAE for our method with those of other implicit solvent models for neutral and cationic solvated molecules in Tab. S2 and Tab. S3, respectively. According to Tab. S2 and Tab. S3, our MPE calculations yield satisfactory results in comparison with the other considered methods.

S2 Mulliken Charges of the $RuPtI_2$ Complex in Various Solvents

Table S4: Calculated Mulliken charges of the $RuPtI_2$ complex in various solvents.

Solvent	Dielectric Constant	Mulliken Charge				
		tpphz	bpy	Pt	I_2	Ru
Gas Phase	1.0000	0.7465	1.1942	0.0601	-0.2780	0.2771
Benzene	2.2706	0.8993	1.2035	0.0801	-0.4626	0.2797
Chlorobenzene	5.6968	0.9951	1.2064	0.0940	-0.5722	0.2767
Dichloroethane	10.1250	1.0294	1.2057	0.0987	-0.6103	0.2765
Acetone	20.4930	1.0541	1.2048	0.1019	-0.6375	0.2768
Ethanol	24.8520	1.0587	1.2054	0.1025	-0.6424	0.2758
Methanol	32.6130	1.0638	1.2053	0.1032	-0.6480	0.2757
Acetonitrile	35.6880	1.0649	1.2043	0.1032	-0.6494	0.2770
DMSO	46.8269	1.0686	1.2046	0.1036	-0.6532	0.2764
Water	78.3553	1.0738	1.2063	0.1046	-0.6589	0.2741

S3 Orbital Transitions within the $RuPtI_2$ Photocatalyst

S3.1 Gas Phase

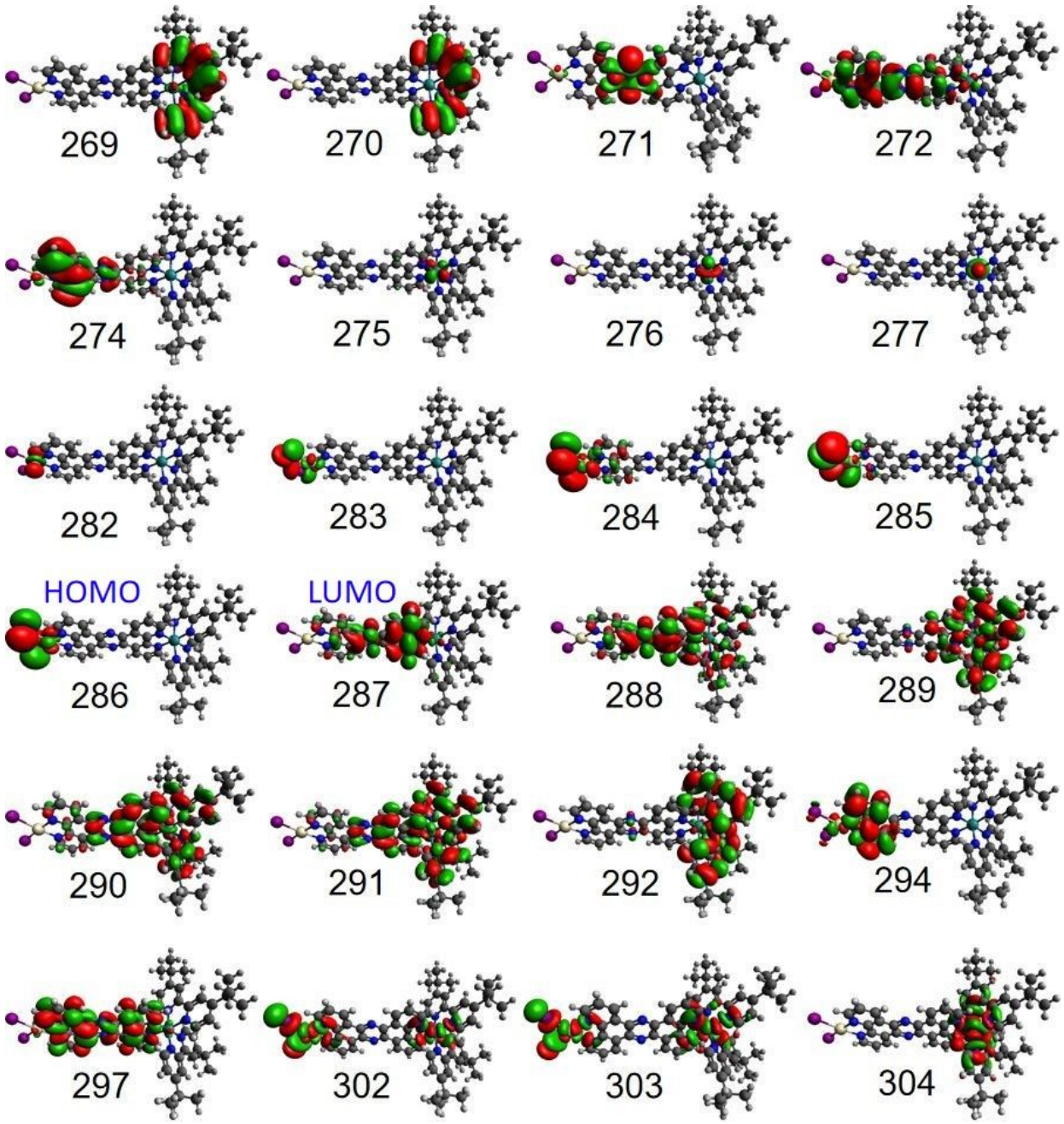

Figure S2: Frontier orbitals of $([(tbbpy)_2Ru(tpphz)PtI_2]^{2+}$ in gas phase.

Table S5: Molecular orbital transitions of the $RuPtI_2$ complex in gas phase

State	**Transition**	**Orbital Transition**	**%**	**VEE (eV)**	**λ (nm)**	**f**
S1	286 → 287	d(Pt),n_I → π^*(tpphz)	92.1620	0.3464	3579.58	0.0000
S7	284 → 287	d(Pt),n_I → π^*(tpphz)	85.0182	0.7416	1671.75	0.0339
S37	284 → 294	d(Pt),n_I → π^*(tpphz)	76.8106	2.0136	615.73	0.1446
	286 → 297	d(Pt),n_I → π^*(tpphz)	21.2709			
S65	275 → 287	d(Ru) → π^*(tpphz)	74.8134	2.7308	454.03	0.1557
S85	275 → 290	d(Ru) → π^*(tpphz),π^*(bpy)	24.2041	2.9535	419.79	0.1406
	275 → 291	d(Ru) → π^*(tpphz),π^*(bpy)	22.6922			
	276 → 289	d(Ru) → π^*(bpy)	44.2665			
S95	276 → 291	d(Ru) → π^*(tpphz),π^*(bpy)	80.5891	3.0849	401.91	0.0937
S131	272 → 287	d(Pt),π^*(tpphz) → π^*(tpphz)	43.4144	3.5962	344.76	0.1603
	272 → 288	d(Pt),π(tpphz) → π^*(tpphz)	27.2366			
	274 → 290	π(tpphz) → π^*(tpphz)	15.8913			
S144	272 → 288	d(Pt),π(tpphz) → π^*(tpphz)	14.1321	3.7728	328.62	0.2479
	279 → 292	d(Pt),n_I → π^*(bpy)	57.7813			
S149	272 → 288	d(Pt),π(tpphz) → π^*(tpphz)	30.6983	3.7916	326.99	0.7257
	274 → 291	π(tpphz) → π^*(tpphz),π^*(bpy)	15.9229			
	279 → 292	d(Pt),n_I → π^*(bpy)	16.3684			
S226	269 → 291	π(bpy) → π^*(tpphz),π^*(bpy)	60.0060	4.5435	272.88	0.3578
	270 → 289	π(bpy) → π^*(bpy)	12.6676			
S228	269 → 289	π(bpy) → π^*(bpy)	28.0486	4.5814	270.62	0.6672
	270 → 291	π(bpy) → π^*(tpphz),π^*(bpy)	28.9424			

Table S6: Molecular orbital singlet-triplet transitions of the $RuPtI_2$ complex in gas phase

State	**Transition**	**Orbital Transition**	**%**	**VEE (eV)**	**f**
T1	286 → 287	d(Pt) → π^*(tpphz)	89.9999	0.3273	0.0000
T7	286 → 289	d(Pt) → π^*(bpy)	93.8943	0.7369	0.0000
T48	277 → 287	d(Ru) → π^*(tpphz)	48.2771	2.2626	0.0000
	277 → 288	d(Ru) → π^*(tpphz)	14.4668		
	277 → 289	d(Ru) → π^*(bpy), π^*(tpphz)	18.5830		
T59	277 → 290	d(Ru) → π^*(tpphz), π^*(bpy)	42.3973	2.4622	0.0000
	277 → 291	d(Ru) → π^*(bpy), π^*(tpphz)	42.3182		
T90	271 → 287	n(tpphz) → π^*(tpphz)	29.1252	2.9245	0.0000
	271 → 288	n(tpphz) → π^*(tpphz)	24.2849		
T112	269 → 290	π(bpy) → π^*(tpphz), π^*(bpy)	10.6750	3.2280	0.0000
	269 → 291	π(bpy) → π^*(bpy), π^*(tpphz)	13.7918		
	270 → 289	π(bpy) → π^*(bpy), π^*(tpphz)	24.7076		
	278 → 291	d(Ru) → π^*(bpy), π^*(tpphz)	11.3478		

S3.2 Benzene

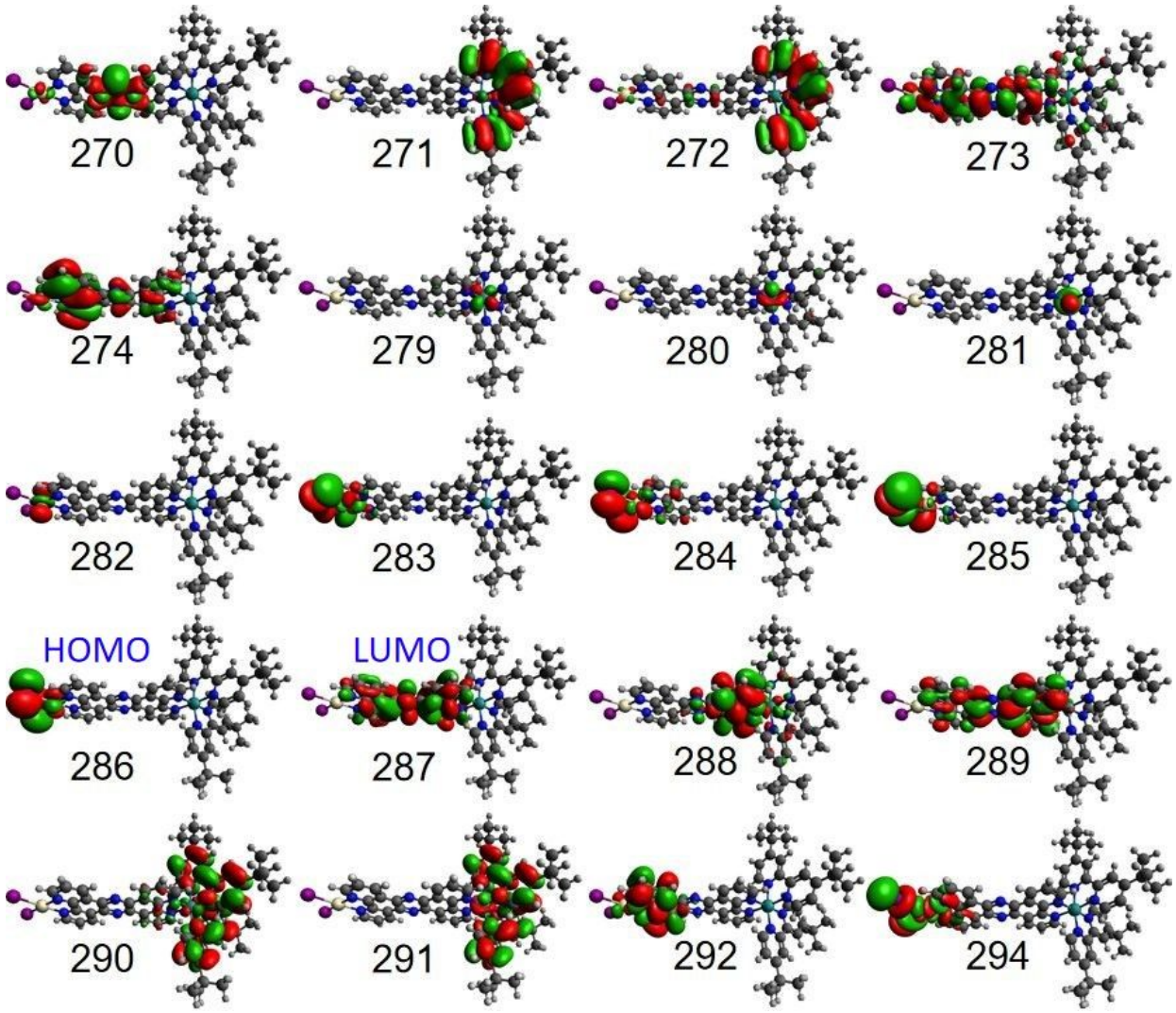

Figure S3: Frontier orbitals of $([(tbbpy)_2Ru(tpphz)PtI_2]^{2+}$ in benzene

Table S7: Molecular orbital transitions of the $RuPtI_2$ complex in benzene

State	**Transition**	**Orbital Transition**	**%**	**VEE (eV)**	**λ (nm)**	**f**
S1	286 → 287	d(Pt),n_I → π^*(tpphz)	98.4850	1.4222	871.80	0.0000
S3	284 → 287	d(Pt),n_I → π^*(tpphz)	98.4654	1.7276	717.65	0.0376
S22	284 → 292	d(Pt),n_I → d*(Pt), π^*(tpphz)	92.1132	2.4154	513.30	0.1475
S28	279 → 287	d(Ru) → π^*(tpphz)	80.9043	2.5719	482.07	0.1134
	279 → 288	d(Ru) → π^*(tpphz)	10.1457			
S45	279 → 288	d(Ru) → π^*(tpphz)	15.5247	2.9221	424.30	0.2227
	279 → 291	d(Ru) → π^*(bpy)	14.4260			
	280 → 289	d(Ru) → π^*(tpphz)	21.8923			
	280 → 291	d(Ru) → π^*(bpy)	18.7897			
S63	276 → 287	π(tpphz),d(Pt),n_I → π^*(tpphz)	13.5314	3.3066	374.96	0.1186
	277 → 287	π(tpphz),d(Pt),n_I → π^*(tpphz)	80.7873			
S81	273 → 287	π(tpphz) → π^*(tpphz)	73.4569	3.6527	339.43	0.2800
	274 → 289	π(tpphz) → π^*(tpphz)	11.6287			
S98	280 → 295	d(Ru) → π^*(bpy)	10.3358	3.8603	321.17	0.1622
	281 → 294	d(Ru) → π^*(tpphz)	19.6151			
	281 → 297	d(Ru) → π^*(bpy)	57.2921			
S108	272 → 287	π(bpy) → π^*(tpphz)	13.7110	3.9576	313.28	0.9685
	274 → 289	π(tpphz) → π^*(tpphz)	42.9924			
	280 → 294	d(Ru) → π^*(tpphz)	10.4278			
S116	274 → 289	π(tpphz) → π^*(tpphz)	10.2016	4.0023	309.78	0.4185
	276 → 292	π(tpphz),d(Pt),n_I → π^*(tpphz)	36.7790			
	277 → 292	π(tpphz),d(Pt),n_I → π^*(tpphz)	13.2499			
	280 → 294	d(Ru) → π^*(tpphz)	22.6491			
S164	271 → 290	π(bpy) → π^*(bpy)	23.7898	4.4458	278.88	0.7919
	272 → 291	π(bpy) → π^*(bpy)	35.7841			
	273 → 291	π(tpphz) → π^*(bpy)	16.0178			
S173	269 → 288	π(tpphz) → π^*(tpphz)	57.1680	4.5877	270.25	0.3658

Table S8: Molecular orbital singlet-triplet transitions of the $RuPtI_2$ complex in benzene

State	**Transition**	**Orbital Transition**	**%**	**Excitation Energy**	**f**
T1	286 → 287	d(Pt) → π^*(tpphz)	97.9720	1.4128	0.0000
T12	286 → 290	d(Pt) → π^*(bpy)	99.4840	2.1321	0.0000
T15	281 → 287	d(Ru) → π^*(tpphz)	25.4513	2.1910	0.0000
	281 → 288	d(Ru) → π^*(tpphz)	54.7016		
T28	281 → 287	d(Ru) → π^*(tpphz)	23.6589	2.4650	0.0000
	281 → 290	d(Ru) → π^*(bpy)	55.7209		
T53	270 → 287	n(tpphz) → π^*(tpphz)	84.3675	2.9427	0.0000
T64	271 → 291	π(bpy) → π^*(bpy)	24.7414	3.2208	0.0000
	272 → 290	π(bpy) → π^*(bpy)	30.0747		

S3.3 Chlorobenzene

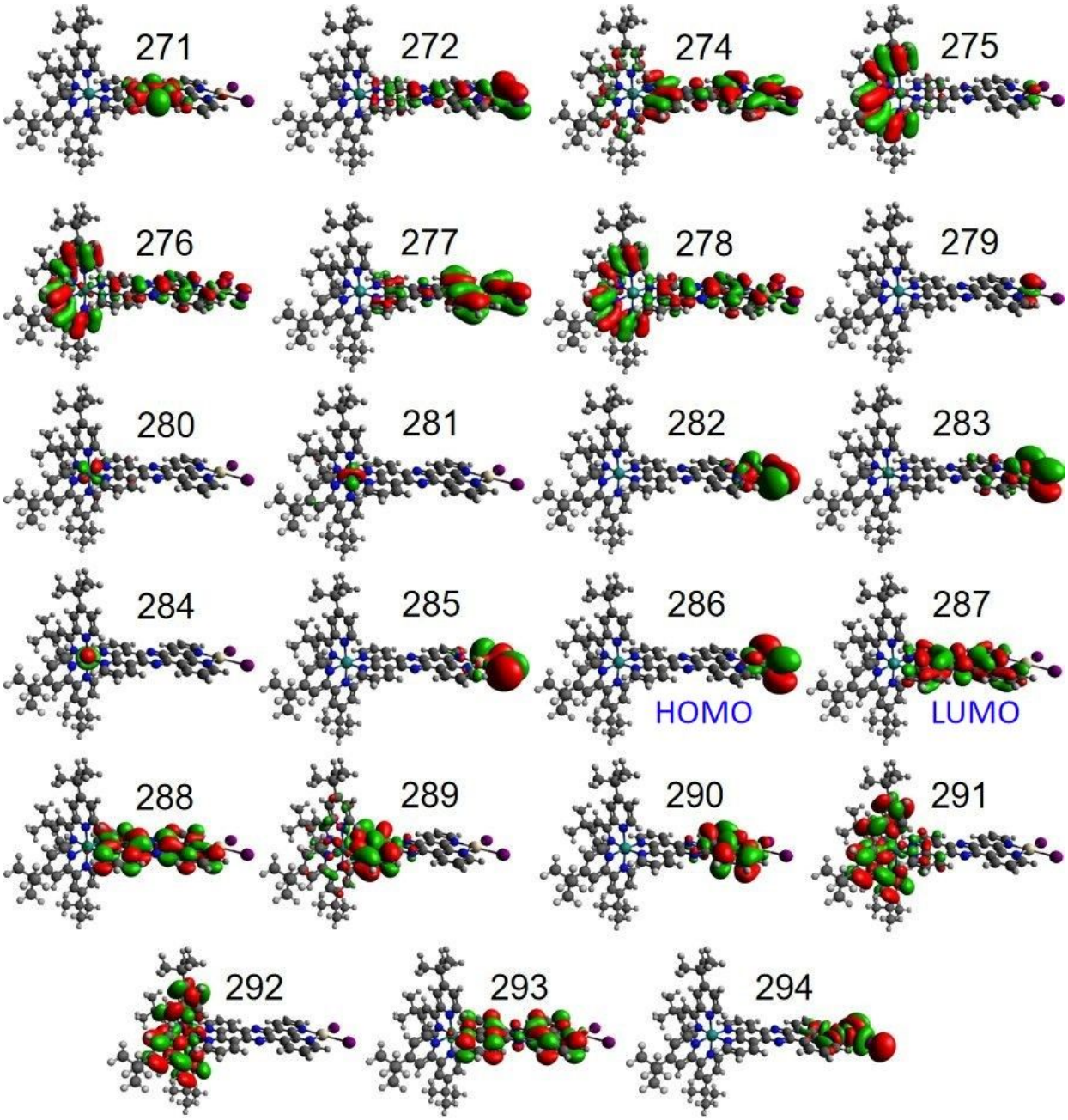

Figure S4: Frontier orbitals of $([(tbbpy)_2Ru(tpphz)PtI_2]^{2+}$ in chlorobenzene.

Table S9: Molecular orbital transition of the $RuPtI_2$ complex in chlorobenzene

State	**Transition**	**Orbital Transition**	**%**	**VEE (eV)**	**λ (nm)**	**f**
S1	286 → 287	d(Pt),n_I → π^*(tpphz)	97.2399	2.1458	577.80	0.0000
S4	280 → 287	d(Ru) → π^*(tpphz)	13.2777	2.3876	519.27	0.1336
	283 → 287	d(Pt),n_I → π^*(tpphz)	83.4580			
S20	280 → 289	d(Ru) → π^*(tpphz)	31.4615	2.7886	444.61	0.1115
	280 → 291	d(Ru) → π^*(bpy)	33.7021			
	281 → 288	d(Ru) → π^*(tpphz)	29.1069			
S25	283 → 290	d(Pt),n_I → π^*(tpphz)	86.6060	2.8502	435.00	0.2030
S30	280 → 292	d(Ru) → π^*(bpy)	70.3867	2.9103	426.02	0.1346
	281 → 291	d(Ru) → π^*(bpy)	26.2160			
S55	276 → 287	π(tpphz), π(bpy) → π^*(tpphz)	26.0353	3.5590	348.37	0.5268
	278 → 287	π(tpphz), π(bpy) → π^*(tpphz)	58.2423			
S80	277 → 288	π(tpphz), d(Pt) → π^*(tpphz)	69.9508	3.9684	312.43	0.7051
S131	272 → 288	d(Pt),n_I → π^*(tpphz)	13.7058	4.4571	278.17	0.8980
	274 → 289	π(tpphz), d(Pt) → π^*(tpphz)	12.8241			
	275 → 291	π(bpy) → π^*(bpy)	16.2188			
	276 → 292	π(tpphz), π(bpy) → π^*(bpy)	15.2849			
	278 → 292	π(tpphz), π(bpy) → π^*(bpy)	20.3828			

Table S10: Molecular orbital singlet-triplet transitions of the $RuPtI_2$ complex in chlorobenzene

State	**Transition**	**Orbital Transition**	**%**	**Excitation Energy**	**f**
T1	286 → 287	d(Pt) → π^*(tpphz)	92.4392	2.1282	0.0000
T2	284 → 287	d(Ru) → π^*(tpphz)	37.3853	2.1722	0.0000
	284 → 289	d(Ru) → π^*(tpphz)	43.8385		
T11	284 → 292	d(Ru) → π^*(bpy)	76.7709	2.4662	0.0000
T37	271 → 287	n(tpphz) → π^*(tpphz)	87.7733	2.9538	0.0000
T39	286 → 291	d(Pt) → π^*(bpy)	99.1852	3.0404	0.0000
T48	275 → 292	π(bpy) → π^*(bpy)	24.5196	3.2194	0.0000
	276 → 291	π(bpy) → π^*(bpy)	18.9334		
	278 → 291	π(bpy) → π^*(bpy)	15.1966		

S3.4 Dichloroethane

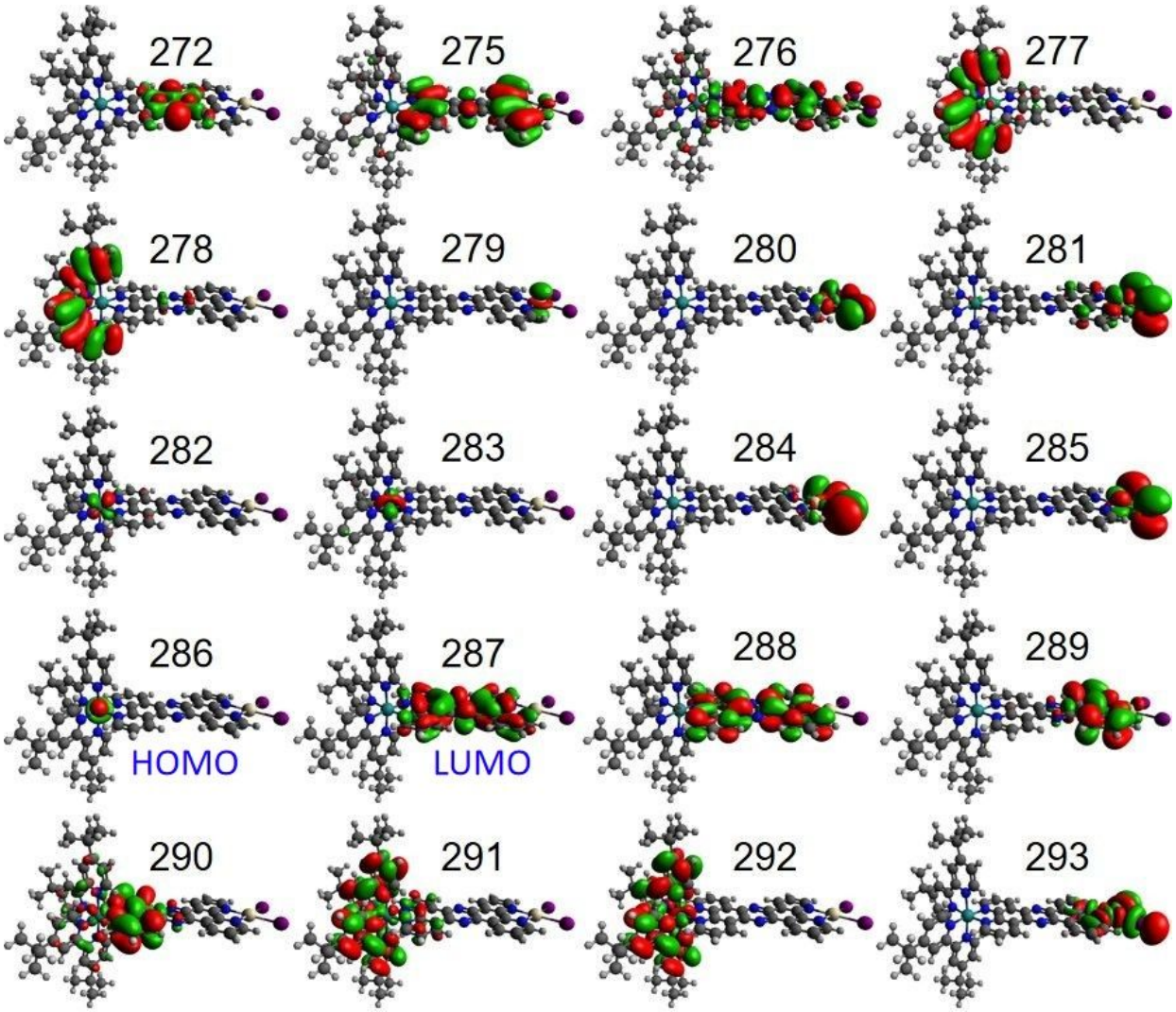

Figure S5: Frontier orbitals of $([(tbbpy)_2Ru(tpphz)PtI_2]^{2+}$ in dichloroethane.

Table S11: Molecular orbital transitions of the $RuPtI_2$ complex in dichloroethane

State	**Transition**	**Orbital Transition**	**%**	**VEE (eV)**	**λ (nm)**	**f**
S1	286 → 287	d(Ru) → π^*(tpphz)	85.0025	2.2129	560.28	0.0004
	286 → 290	d(Ru) → π^*(tpphz)	12.4331			
S3	282 → 287	d(Ru) → π^*(tpphz)	95.1565	2.3748	522.08	0.0755
S20	282 → 288	d(Ru) → π^*(tpphz)	14.9233	2.8042	442.14	0.0648
	282 → 292	d(Ru) → π^*(bpy)	21.9307			
	283 → 291	d(Ru) → π^*(bpy)	55.2868			
S22	282 → 290	d(Ru) → π^*(tpphz)	14.1140	2.8655	432.68	0.1799
	282 → 291	d(Ru) → π^*(bpy)	39.8707			
	283 → 292	d(Ru) → π^*(bpy)	37.1591			
S23	282 → 292	d(Ru) → π^*(bpy)	68.4544	2.9077	426.40	0.1389
	283 → 291	d(Ru) → π^*(bpy)	28.8891			
S26	281 → 289	d(Pt),n_I → π^*(tpphz)	75.3231	3.0192	410.65	0.1157
S50	276 → 287	π(tpphz) → π^*(tpphz)	67.6191	3.5889	345.47	0.4606
	278 → 287	π(bpy) → π^*(tpphz)	16.1960			
S78	275 → 288	π(tpphz) → π^*(tpphz)	44.7401	4.0169	308.66	1.0033
	276 → 289	π(tpphz) → π^*(tpphz)	24.0291			
S122	277 → 291	π(bpy) → π^*(bpy)	24.5715	4.4621	277.86	1.0013
	278 → 292	π(bpy) → π^*(bpy)	48.3380			

Table S12: Molecular orbital singlet-triplet transitions of the $RuPtI_2$ complex in dichloroethane

State	**Transition**	**Orbital Transition**	**%**	**VEE (eV)**	**f**
T1	286 → 287	d(Ru) → π^*(tpphz)	61.7249	2.1507	0.0000
	286 → 290	d(Ru) → π^*(tpphz)	27.1422		
T7	285 → 287	d(Pt) → π^*(tpphz)	79.5187	2.3702	0.0000
	285 → 289	d(Pt) → π^*(tpphz)	13.1092		
T9	286 → 290	d(Ru) → π^*(tpphz)	12.2889	2.4635	0.0000
	286 → 291	d(Ru) → π^*(bpy)	72.9463		
T32	272 → 287	n(tpphz) → π^*(tpphz)	73.9960	2.9590	0.0000
	286 → 289	d(Ru) → π^*(tpphz)	16.8769		
T43	277 → 292	π(bpy) → π^*(bpy)	26.6830	3.2163	0.0000
	278 → 291	π(bpy) → π^*(tpphz)	32.4157		
T47	285 → 291	d(Pt) → π^*(bpy)	99.2049	3.3674	0.0000

S3.5 Acetone

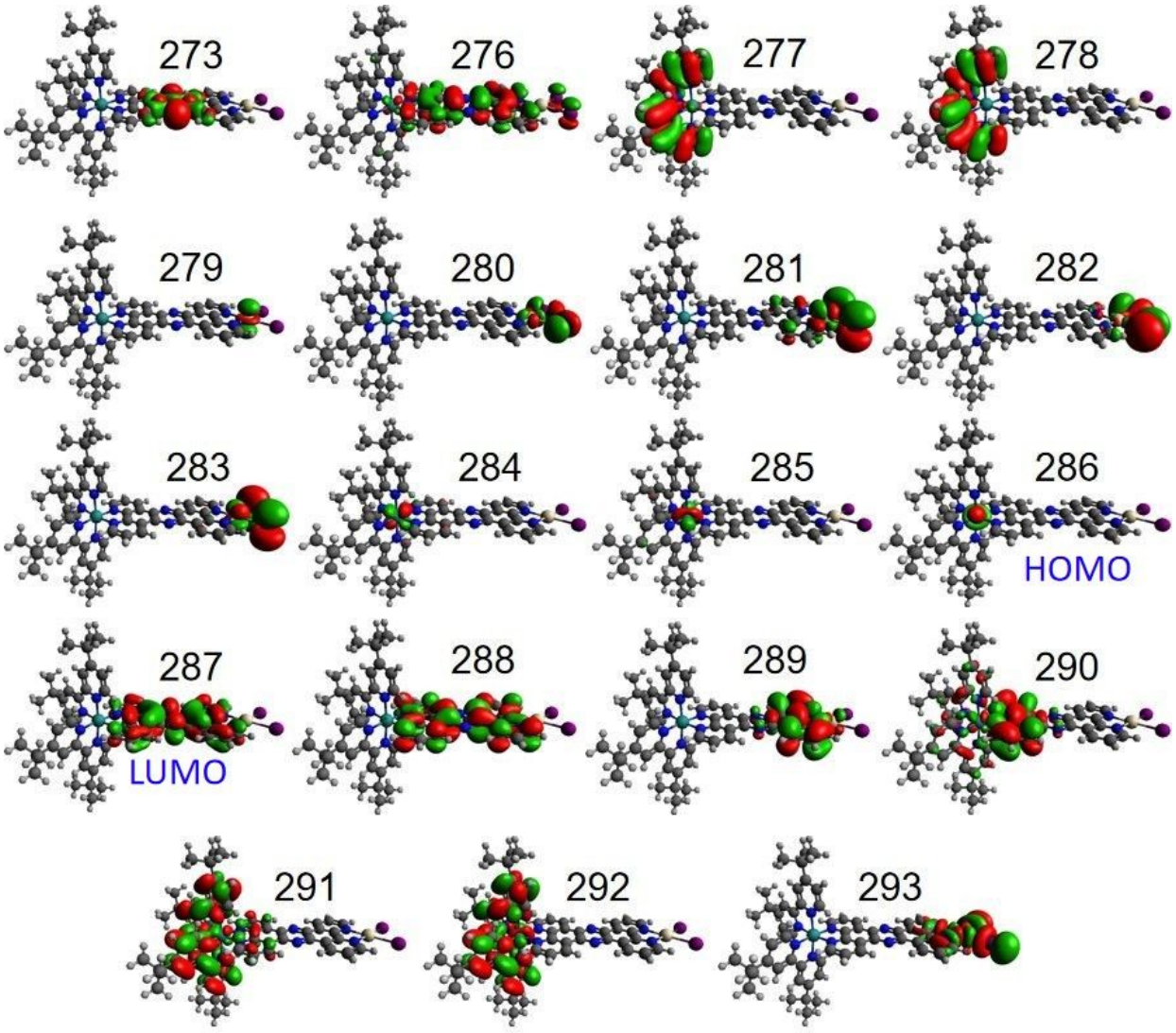

Figure S6: Frontier orbitals of $[(tbbpy)_2Ru(tpphz)PtI_2]^{2+}$ in acetone

Table S13: Molecular orbital transition of the $RuPtI_2$ complex in acetone

State	**Transition**	**Orbital Transition**	**%**	**VEE (eV)**	**λ (nm)**	**f**
S1	286 → 287	d(Ru) → π^*(tpphz)	88.4902	2.1781	569.22	0.0004
S3	285 → 287	d(Ru) → π^*(tpphz)	90.9172	2.3402	529.80	0.0605
S13	284 → 290	d(Ru) → π^*(tpphz)	57.0654	2.7680	447.92	0.2274
	284 → 291	d(Ru) → π^*(bpy)	24.9571			
S19	284 → 290	d(Ru) → π^*(tpphz)	14.4948	2.8641	432.88	0.1367
	284 → 291	d(Ru) → π^*(bpy)	39.8171			
	285 → 292	d(Ru) → π^*(bpy)	36.3105			
S21	284 → 292	d(Ru) → π^*(bpy)	66.0307	2.9075	426.43	0.1415
	285 → 291	d(Ru) → π^*(bpy)	31.5313			
S31	281 → 289	d(Pt),n_I → π^*(tpphz)	82.9730	3.1489	393.74	0.0969
	283 → 288	d(Pt),n_I → π^*(tpphz)	10.3704			
S46	276 → 287	π(tpphz) → π^*(tpphz)	26.3422	3.5947	344.91	0.3036
	285 → 294	d(Ru) → π^*(tpphz)	56.2542			
S76	275 → 288	π(tpphz) → π^*(tpphz)	19.7758	4.0203	308.39	0.5177
	276 → 289	π(tpphz) → π^*(tpphz)	56.1652			
S80	275 → 288	π(tpphz) → π^*(tpphz)	25.9863	4.0584	305.50	0.8026
	276 → 289	π(tpphz) → π^*(tpphz)	20.4429			
	277 → 288	π(bpy) → π^*(tpphz)	15.1514			
S115	277 → 291	π(bpy) → π^*(bpy)	26.7005	4.4789	276.82	0.9861
	278 → 292	π(bpy) → π*(bpy)	46.8686			

Table S14: Molecular orbital singlet-triplet transitions of the $RuPtI_2$ complex in acetone

State	**Transition**	**Orbital Transition**	**%**	**VEE (eV)**	**f**
T1	286 → 287	d(Ru) → π^*(tpphz)	61.7249	2.1297	0.0000
	286 → 290	d(Ru) → π^*(tpphz)	27.1422		
T8	286 → 290	d(Ru) → π^*(tpphz)	11.8477	2.4572	0.0000
	286 → 291	d(Ru) → π^*(bpy)	73.5102		
T10	283 → 287	d(Pt) → π^*(tpphz)	43.1112	2.5208	0.0000
	283 → 289	d(Pt) → π^*(tpphz)	18.7627		
	285 → 290	d(Ru) → π^*(tpphz)	14.6113		
T31	273 → 287	n(tpphz) → π^*(tpphz)	61.1618	2.9670	0.0000
	280 → 287	d(Pt) → π^*(tpphz)	25.6385		
T39	277 → 292	π(bpy) → π^*(bpy)	27.9303	3.2135	0.0000
	278 → 291	π(bpy) → π^*(bpy)	33.1542		
T60	283 → 291	d(Pt) → π^*(bpy)	99.1485	3.6044	0.0000

S3.6 Ethanol

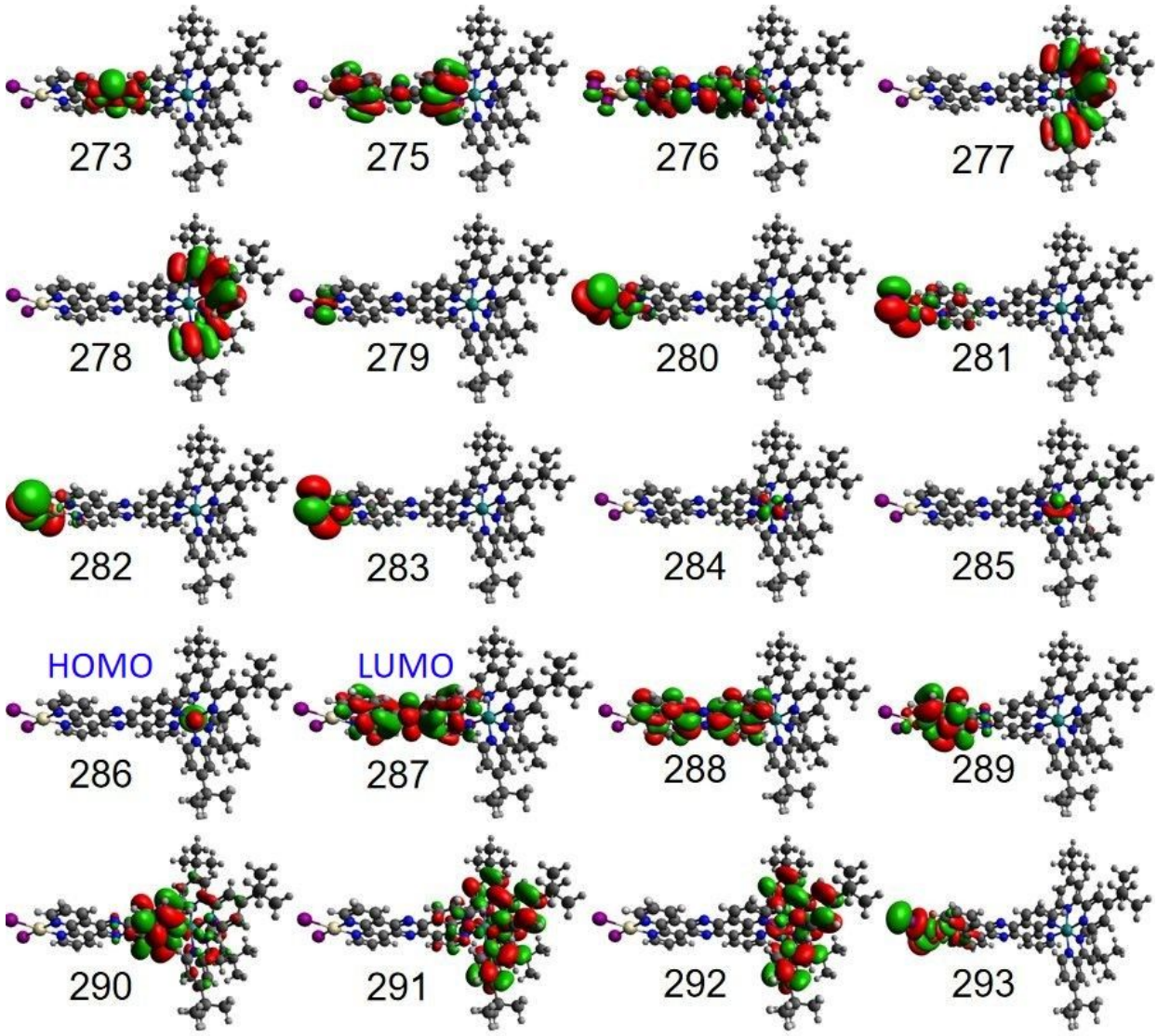

Figure S7: Frontier orbitals of $([(tbbpy)_2Ru(tpphz)PtI_2]^{2+}$ in ethanol

Table S15: Molecular orbital transition of the $RuPtI_2$ complex in ethanol

State	**Transition**	**Orbital Transition**	**%**	**VEE (eV)**	**λ (nm)**	**f**
S1	286 → 287	d(Ru) → π^*(tpphz)	89.0579	2.1719	570.85	0.0005
S3	284 → 287	d(Ru) → π^*(tpphz)	95.8697	2.3305	532.00	0.0588
S13	284 → 290	d(Ru) → π^*(tpphz)	61.4054	2.7646	448.47	0.1968
	284 → 291	d(Ru) → π^*(bpy)	26.3785			
S17	281 → 287	d(Pt),n_I → π^*(tpphz)	85.0625	2.8257	438.78	0.1462
S20	284 → 292	d(Ru) → π^*(bpy)	65.9342	2.9053	426.76	0.1428
	285 → 291	d(Ru) → π^*(bpy)	31.6362			
S33	281 → 289	d(Pt),n_I → π^*(tpphz)	14.8218	3.1773	390.22	0.0962
	282 → 293	n_I → π^*(tpphz),d*(Pt),n_I^*	80.7212			
S49	276 → 287	π(tpphz) → π^*(tpphz)	54.6932	3.6082	343.62	0.2626
	278 → 287	π(bpy) → π^*(tpphz)	19.6690			
	285 → 294	d(Ru) → π^*(tpphz)	10.4333			
S79	275 → 288	π(tpphz) → π^*(tpphz)	29.3072	4.0555	305.72	0.8908
	276 → 289	π(tpphz) → π^*(tpphz)	15.9726			
	277 → 288	π(bpy) → π^*(tpphz)	18.1612			
S114	277 → 291	π(bpy) → π^*(bpy)	26.7634	4.4799	276.76	0.9883
	278 → 292	π(bpy) → π^*(bpy)	46.5477			

Table S16: Molecular orbital singlet-triplet transitions of the $RuPtI_2$ complex in ethanol

State	**Transition**	**Orbital Transition**	**%**	**VEE (eV)**	**f**
T1	286 → 287	d(Ru) → π^*(tpphz)	63.7591	2.1257	0.0000
	286 → 290	d(Ru) → π^*(tpphz)	25.5212		
T8	286 → 290	d(Ru) → π^*(tpphz)	12.6948	2.4559	0.0000
	286 → 291	d(Ru) → π^*(bpy)	73.0188		
T12	283 → 287	d(Pt) → π^*(tpphz)	33.5888	2.5352	0.0000
	283 → 289	d(Pt) → π^*(tpphz)	19.2609		
	285 → 290	d(Ru) → π^*(tpphz)	15.0470		
T29	273 → 287	n(tpphz) → π^*(tpphz)	70.6718	2.9577	0.0000
	285 → 289	d(Ru) → π^*(tpphz)	11.2822		
T39	277 → 292	π(bpy) → π^*(bpy)	27.8736	3.2141	0.0000
	278 → 291	π(bpy) → π^*(bpy)	32.9802		
T67	283 → 291	d(Pt) → π^*(bpy)	99.1429	3.6474	0.0000

S3.7 Methanol

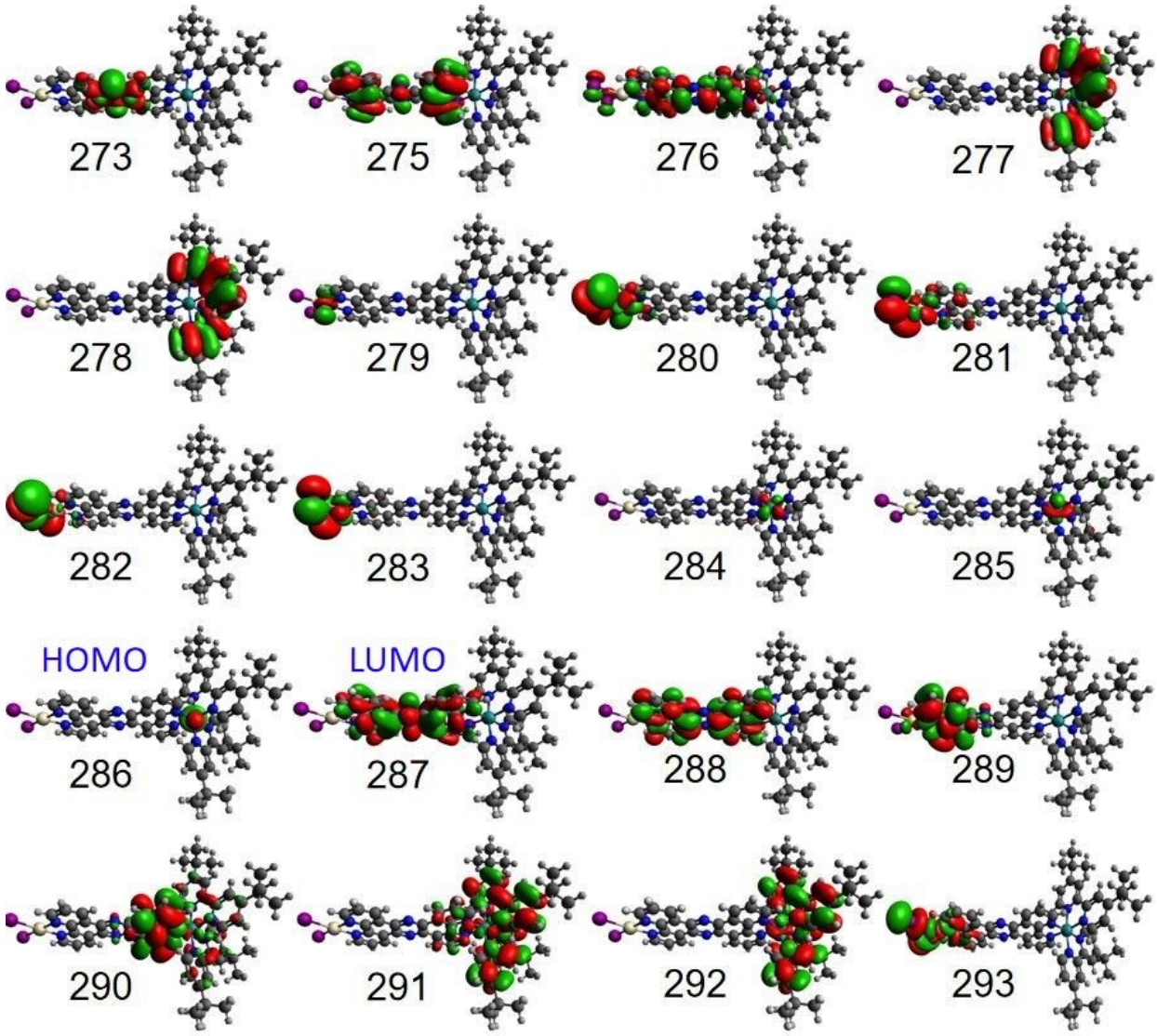

Figure S8: Frontier orbitals of $([(tbbpy)_2Ru(tpphz)PtI_2]^{2+}$ in methanol

Table S17: Molecular orbital transitions of the $RuPtI_2$ complex in methanol

State	**Transition**	**Orbital Transition**	**%**	**VEE (eV)**	**λ (nm)**	**f**
S1	286 → 287	d(Ru) → π^*(tpphz)	89.5925	2.1643	572.86	0.0005
S3	284 → 287	d(Ru) → π^*(tpphz)	95.9583	2.3224	533.86	0.0561
S13	284 → 290	d(Ru) → π^*(tpphz)	62.8791	2.7638	448.60	0.1809
	284 → 291	d(Ru) → π^*(bpy)	26.8249			
S17	281 → 287	d(Pt),n_I → π^*(tpphz)	44.9409	2.8501	435.02	0.2613
	284 → 291	d(Ru) → π^*(bpy)	25.1894			
	285 → 292	d(Ru) → π^*(bpy)	20.1244			
S20	284 → 292	d(Ru) → π^*(bpy)	65.0347	2.9055	426.73	0.1429
	285 → 291	d(Ru) → π^*(bpy)	32.4786			
S33	281 → 289	d(Pt),n_I → π^*(tpphz)	77.6557	3.1993	387.54	0.1395
	283 → 288	d(Pt),n_I → π^*(tpphz)	13.0050			
S49	276 → 287	π(tpphz) → π^*(tpphz)	45.4371	3.6103	343.42	0.2442
	278 → 287	π(bpy) → π^*(tpphz)	20.1854			
	279 → 288	d(Pt) → π^*(tpphz)	19.4301			
S77	275 → 288	π(tpphz) → π^*(tpphz)	31.4456	4.0539	305.84	0.9671
	277 → 288	π(bpy) → π^*(tpphz)	23.4325			
S114	277 → 291	π(bpy) → π^*(bpy)	27.2130	4.4865	276.35	0.9584
	278 → 292	π(bpy) → π^*(bpy)	45.7886			

Table S18: Molecular orbital singlet-triplet transitions of the $RuPtI_2$ complex in methanol

State	**Transition**	**Orbital Transition**	**%**	**VEE (eV)**	**f**
T1	286 → 287	d(Ru) → π^*(tpphz)	66.0537	2.1205	0.0000
	286 → 290	d(Ru) → π^*(tpphz)	23.8326		
T8	286 → 290	d(Ru) → π^*(tpphz)	13.2088	2.4545	0.0000
	286 → 291	d(Ru) → π^*(bpy)	72.7532		
T13	283 → 287	d(Pt) → π^*(tpphz)	18.4334	2.5470	0.0000
	283 → 289	d(Pt) → π^*(tpphz)	14.1906		
	284 → 288	d(Ru) → π^*(tpphz)	11.2642		
	285 → 290	d(Ru) → π^* (tpphz)	19.1185		
	285 → 291	d(Ru) → π^* (Ru)	10.6002		
T31	273 → 287	n(tpphz) → π^*(tpphz)	85.2296	2.9616	0.0000
T38	277 → 292	π(bpy) → π^*(bpy)	27.9483	3.2137	0.0000
	278 → 291	π(bpy) → π^*(bpy)	32.9055		
T66	283 → 291	d(Pt) → π^*(bpy)	98.1372	3.6963	0.0000

S3.8 Acetonitrile

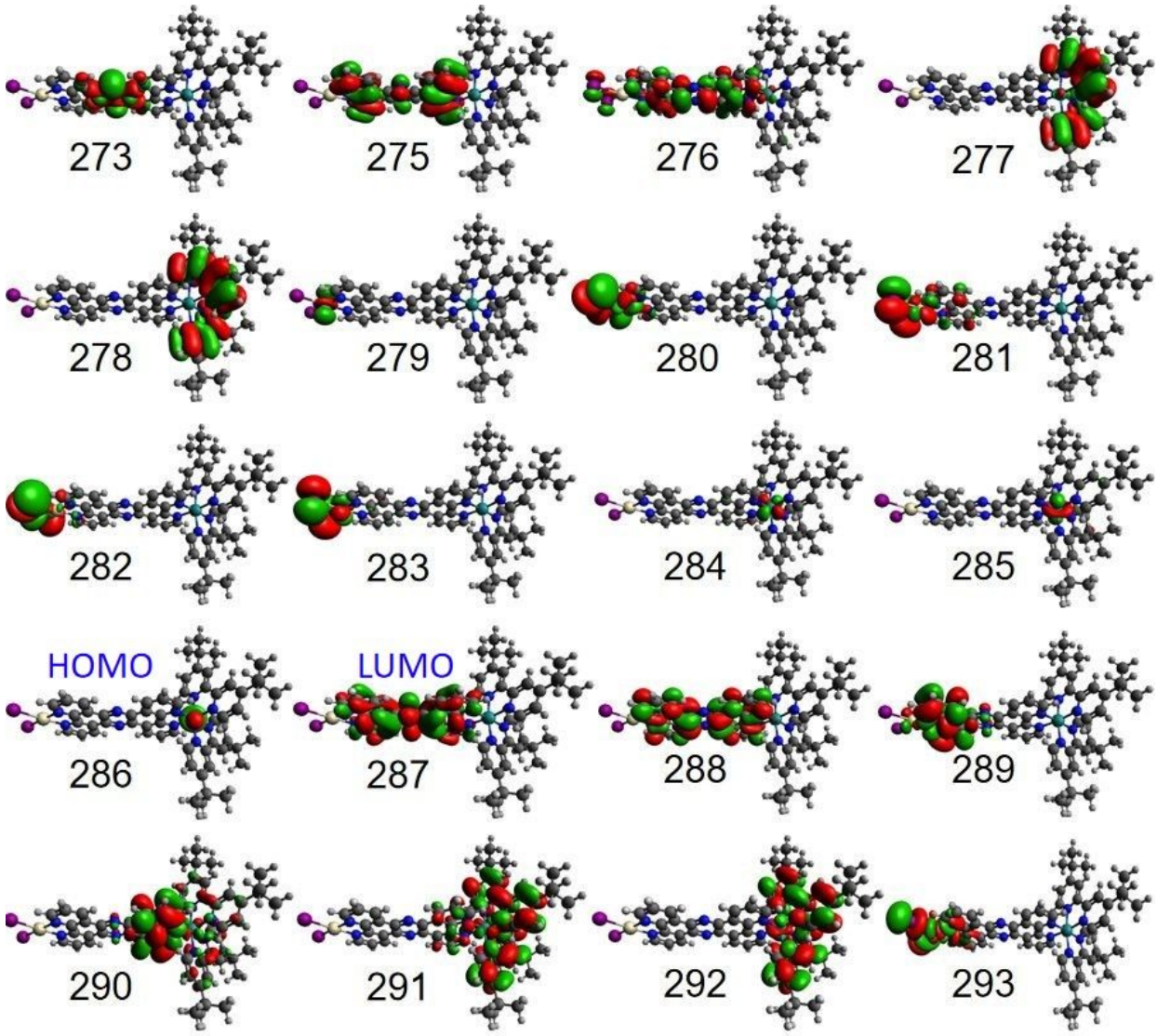

Figure S9: Frontier orbitals of $([(tbbpy)_2Ru(tpphz)PtI_2]^{2+}$ in acetonitrile

Table S19: Molecular orbital transitions of the $RuPtI_2$ complex in acetonitrile

State	**Transition**	**Orbital Transition**	**%**	**VEE (eV)**	**λ (nm)**	**f**
S1	286 → 287	d(Ru) → π^*(tpphz)	89.6541	2.1618	573.51	0.0005
S3	284 → 287	d(Ru) → π^*(tpphz)	95.9223	2.3235	533.61	0.0562
S13	284 → 290	d(Ru) → π^*(tpphz)	63.7298	2.7660	448.24	0.1834
	284 → 291	d(Ru) → π^*(bpy)	26.3480			
S17	281 → 287	d(Pt), n_I → π^*(tpphz)	26.7414	2.8541	434.40	0.2625
	284 → 291	d(Ru) → π^*(bpy)	33.4726			
	285 → 292	d(Ru) → π^*(bpy)	27.4096			
S20	284 → 292	d(Ru) → π^*(bpy)	64.8547	2.9063	426.60	0.1441
	285 → 291	d(Ru) → π^*(bpy)	32.6642			
S33	281 → 289	d(Pt), n_I → π^*(tpphz)	80.1986	3.2061	386.72	0.1325
	283 → 288	d(Pt), n_I → π^*(tpphz)	13.5846			
S48	276 → 287	π(tpphz) → π^*(tpphz)	56.8391	3.6087	343.57	0.3019
	278 → 287	π(bpy) → π^*(tpphz)	25.0717			
S77	275 → 288	π(tpphz) → π^*(tpphz)	32.1682	4.0511	306.05	0.9707
	277 → 288	π(bpy) → π^*(tpphz)	23.5120			
S112	277 → 291	π(bpy) → π^*(bpy)	27.0083	4.4815	276.66	0.9648
	278 → 292	π(bpy) → π^*(bpy)	45.9572			
S199	270 → 290	d(Pt), n_I → π^*(tpphz)	10.6463	5.2114	237.91	0.2970
	271 → 293	d(Pt),n_I → d*(Pt),n_I^*	35.6691			
	274 → 294	π(tpphz),d(Pt),n_I → π^*(tpphz)	29.0474			

Table S20: Molecular orbital singlet-triplet transitions of the $RuPtI_2$ complex in acetonitrile

State	**Transition**	**Orbital Transition**	**%**	**VEE (eV)**	**f**
T1	286 → 287	d(Ru) → π^*(tpphz)	66.6366	2.1186	0.0000
	286 → 290	d(Ru) → π^*(tpphz)	23.5792		
T8	286 → 290	d(Ru) → π^*(tpphz)	12.7856	2.4544	0.0000
	286 → 291	d(Ru) → π^*(bpy)	73.2365		
T16	283 → 287	d(Pt) → π^*(tpphz)	32.2388	2.5505	0.0000
	283 → 289	d(Pt) → π^*(tpphz)	14.0333		
	284 → 288	d(Pt) → π^*(tpphz)	26.1567		
	285 → 291	d(Ru) → π^* (bpy)	13.3945		
T31	273 → 287	n(tpphz) → π^*(tpphz)	86.2037	2.9621	0.0000
T38	277 → 292	π(bpy) → π^*(bpy)	28.1610	3.2122	0.0000
	278 → 291	π(bpy) → π^*(bpy)	33.0777		
T67	283 →291	d(Pt) → π^*(bpy)	99.1232	3.7098	0.0000

S3.9 DMSO

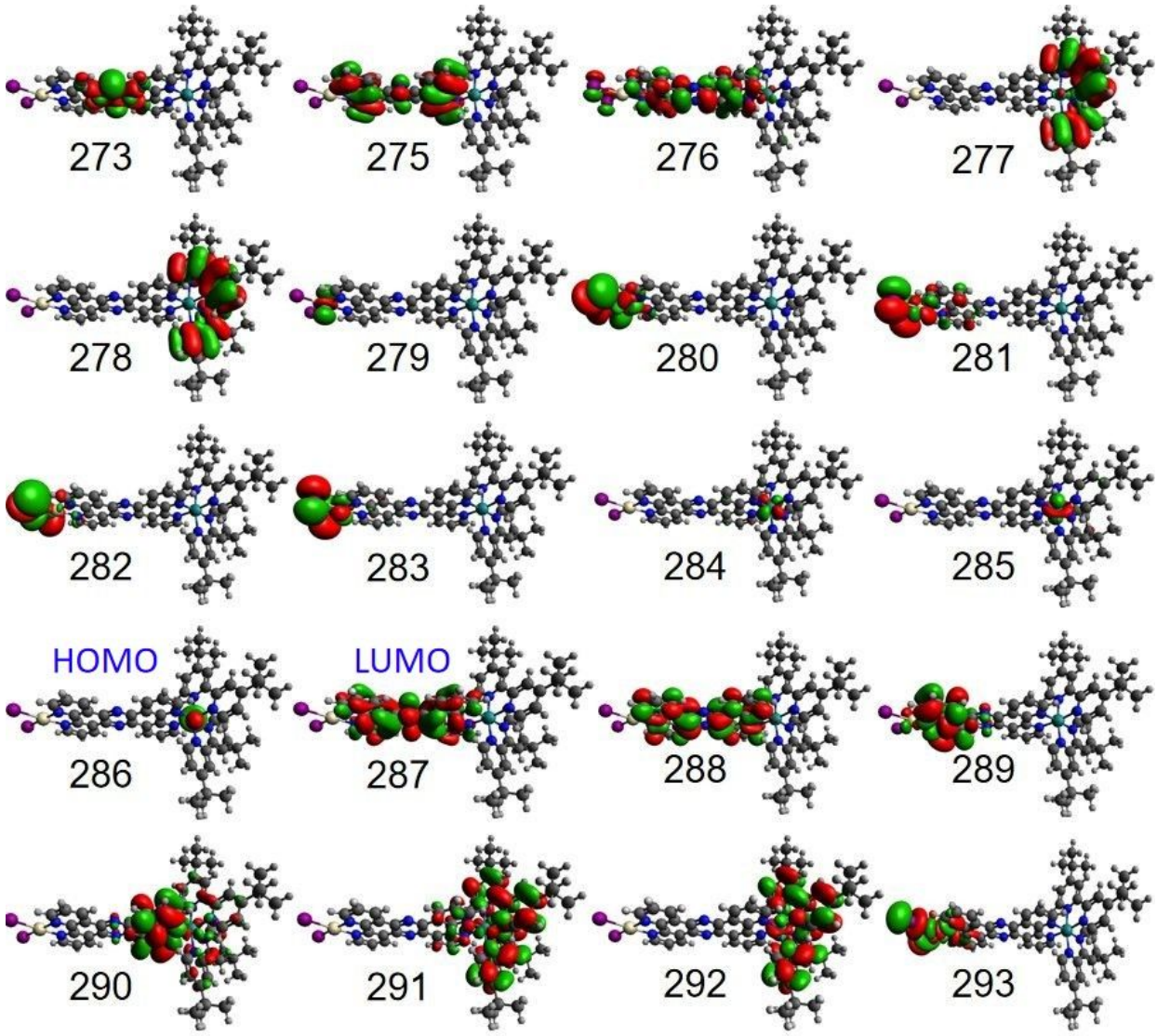

Figure S10: Frontier orbitals of $([(tbbpy)_2Ru(tpphz)PtI_2]^{2+}$ in DMSO

Table S21: Molecular orbital transitions of the $RuPtI_2$ complex in DMSO

State	**Transition**	**Orbital Transition**	**%**	**VEE (eV)**	**λ (nm)**	**f**
S1	286 → 287	d(Ru) → π^*(tpphz)	90.0240	2.1563	574.99	0.0005
S3	284 → 287	d(Ru) → π^*(tpphz)	95.9251	2.3170	535.11	0.0570
S12	284 → 290	d(Ru) → π^*(tpphz)	66.1043	2.7620	448.89	0.1923
	284 → 291	d(Ru) → π^*(bpy)	24.1679			
S17	284 → 291	d(Ru) → π^*(bpy)	43.3176	2.8549	434.28	0.2207
	285 → 292	d(Ru) → π^*(bpy)	35.3775			
S20	284 → 292	d(Ru) → π^*(bpy)	65.6085	2.9032	427.06	0.1478
	285 → 291	d(Ru) → π^*(bpy)	31.9424			
S33	281 → 289	d(Pt),n_I → π^*(tpphz)	80.6653	3.2209	384.94	0.1244
	283 → 288	d(Pt),n_I → π^*(tpphz)	14.8774			
S48	276 → 287	π(tpphz) → π^*(tpphz)	58.1473	3.6052	343.91	0.3302
	278 → 287	π(bpy) → π^*(tpphz)	26.2711			
S76	275 → 288	π(tpphz) → π^*(tpphz)	35.0167	4.0442	306.57	1.0046
	277 → 288	π(bpy) → π^*(tpphz)	22.9029			
S108	277 → 292	π(bpy) → π^*(bpy)	77.1754	4.4482	278.73	0.2591
S111	277 → 291	π(bpy) → π^*(bpy)	26.0916	4.4686	277.46	1.0012
	278 → 292	π(bpy) → π^*(bpy)	46.5709			
S200	271 → 293	d(Pt),n_I → d*(Pt),n_I^*	46.5130	5.3133	237.82	0.3813
	274 → 294	π(tpphz) → π^*(tpphz)	25.7059			

Table S22: Molecular orbital singlet-triplet transitions of the $RuPtI_2$ complex in DMSO

State	**Transition**	**Orbital Transition**	**%**	**VEE (eV)**	**f**
T1	286 → 287	d(Ru) → π^*(tpphz)	68.2509	2.1148	0.0000
	286 → 290	d(Ru) → π^*(tpphz)	22.3593		
T8	286 → 290	d(Ru) → π^*(tpphz)	13.1379	2.4533	0.0000
	286 → 291	d(Ru) → π^*(bpy)	73.0429		
T16	283 → 287	d(Pt) → π^*(tpphz)	35.7790	2.6141	0.0000
	283 → 289	d(Pt) → π^*(tpphz)	19.9737		
	284 → 289	d(Pt) → π^*(tpphz)	23.8354		
T30	273 → 287	n(tpphz) → π^*(tpphz)	87.6620	2.9633	0.0000
T38	277 → 292	π(bpy) → π^*(bpy)	28.2001	3.2126	0.0000
	278 → 291	π(bpy) → π^*(bpy)	32.9802		
T70	283 →291	d(Pt) → π^*(bpy)	99.1429	3.7449	0.0000

S3.10 Water

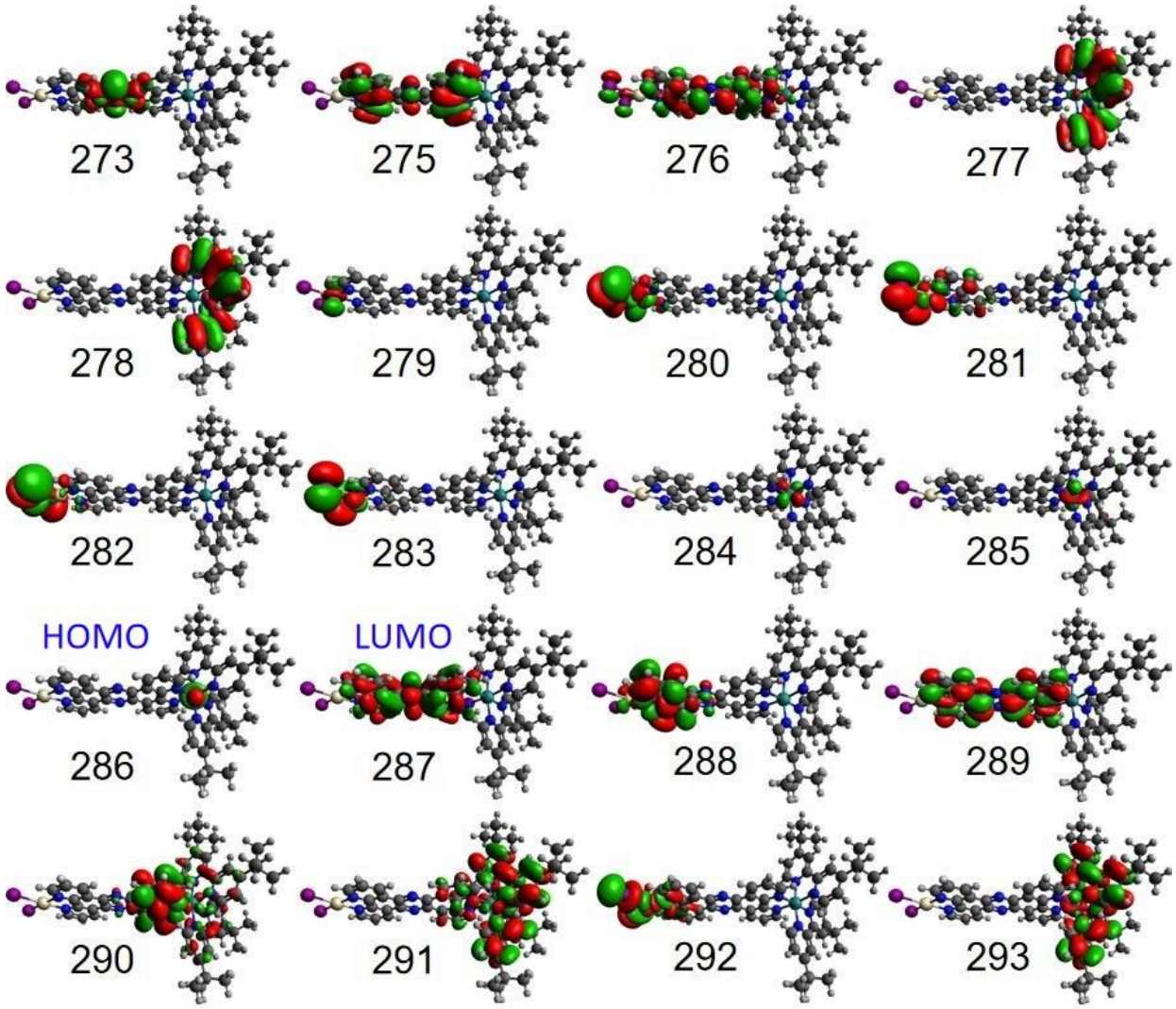

Figure S11: Frontier orbitals of $([(tbbpy)_2Ru(tpphz)PtI_2]^{2+}$ in water

Table S23: Molecular orbital singlet-singlet transitions of the $RuPtI_2$ complex in water

State	**Transition**	**Orbital Transition**	**%**	**VEE (eV)**	**λ (nm)**	**f**
S1	286 → 287	d(Ru) → π^*(tpphz)	90.5481	2.1536	575.70	0.0005
S2	284 → 287	d(Ru) → π^*(tpphz)	96.1080	2.2974	539.67	0.0529
S12	284 → 290	d(Ru) → π^*(tpphz)	65.9940	2.7498	450.88	0.1771
	284 → 291	d(Ru) → π^*(bpy)	24.2974			
S17	284 → 290	d(Ru) → π^*(tpphz)	10.3349	2.8508	434.91	0.1968
	284 → 291	d(Ru) → π^*(bpy)	43.4629			
	285 → 293	d(Ru) → π^*(bpy)	36.7499			
S20	284 → 293	d(Ru) → π^*(bpy)	64.2456	2.8988	427.71	0.1466
	285 → 291	d(Ru) → π^*(bpy)	32.6173			
S33	281 → 288	d(Pt),n_I → π^*(tpphz)	78.1550	3.2475	381.78	0.1189
	283 → 289	d(Pt),n_I → π^*(tpphz)	17.4085			
S48	276 → 287	π(tpphz) → π^*(tpphz)	50.6058	3.6094	343.50	0.2911
	278 → 287	π(bpy) → π^*(tpphz)	36.1590			
S75	275 → 289	π(tpphz) → π^*(tpphz)	30.9386	4.0466	306.39	0.9673
	277 → 289	π(bpy) → π^*(tpphz)	32.1313			
S111	277 → 291	π(bpy) → π^*(bpy)	27.6188	4.4884	276.23	0.9546
	278 → 293	π(bpy) → π^*(bpy)	45.0737			

Table S24: Molecular orbital singlet-triplet transitions of the $RuPtI_2$ complex in water

State	**Transition**	**Orbital Transition**	**%**	**VEE (eV)**	**f**
T1	286 → 287	d(Ru) → π^*(tpphz)	70.0597	2.1145	0.0000
	286 → 290	d(Ru) → π^*(tpphz)	20.3407		
T8	286 → 290	d(Ru) → π^*(tpphz)	17.3107	2.4548	0.0000
	286 → 291	d(Ru) → π^*(bpy)	68.5644		
T16	283 → 287	d(Pt) → π^*(tpphz)	34.8462	2.6246	0.0000
	283 → 288	d(Pt) → π^*(tpphz)	25.3315		
	284 → 289	d(Pt) → π^*(tpphz)	18.2686		
T30	273 → 287	n(tpphz) → π^*(tpphz)	88.1287	2.9635	0.0000
T38	277 → 293	π(bpy) → π^*(bpy)	27.7274	3.2149	0.0000
	278 → 291	π(bpy) → π^*(bpy)	32.2019		
T72	283 → 291	d(Pt) → π^*(bpy)	98.2998	3.7924	0.0000

S4 Orbital Transitions of the $RuPdCl_2$ Photocatalyst

S4.1 Gas Phase

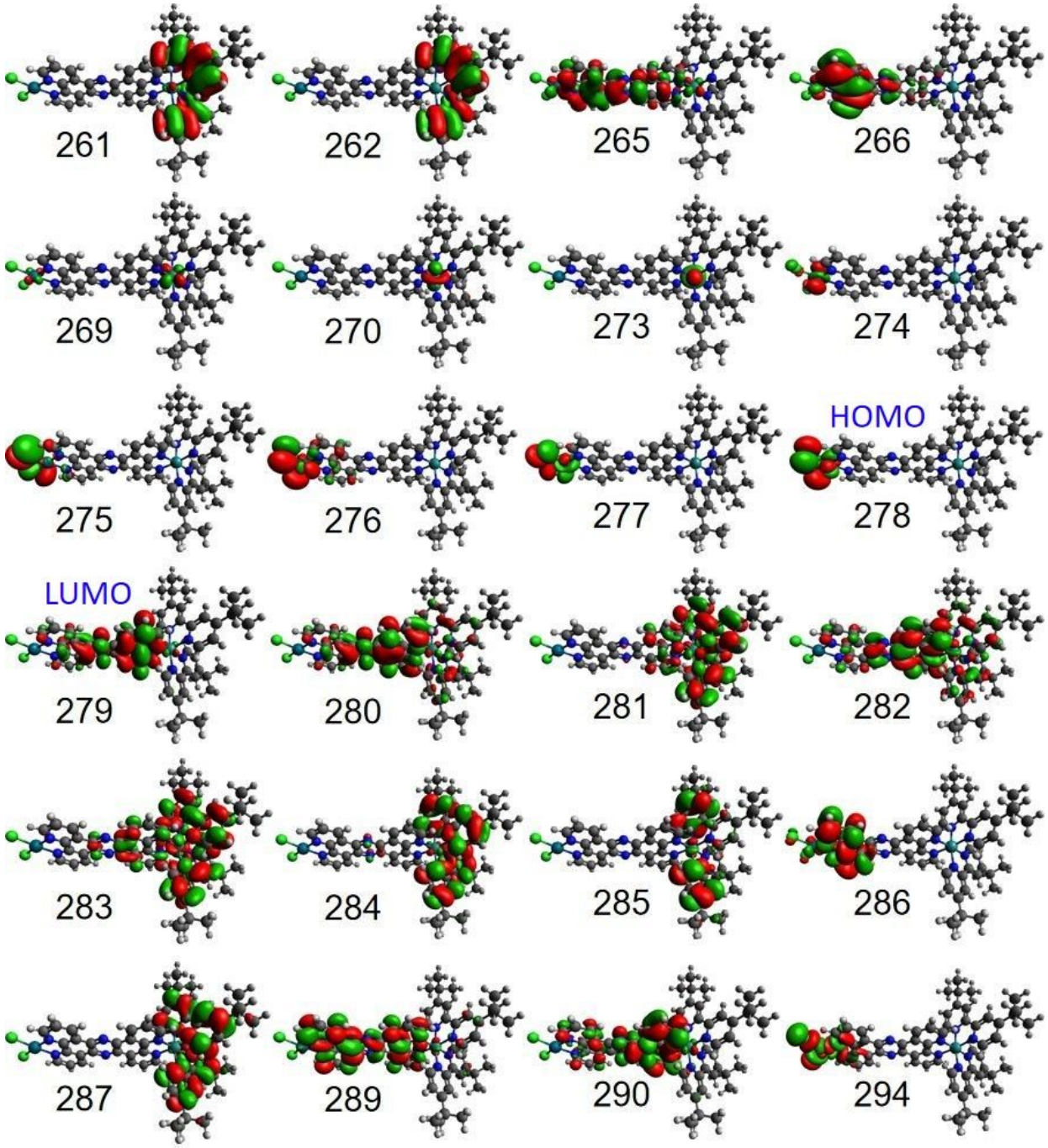

Figure S12: Frontier orbitals of $([(tbbpy)_2Ru(tpphz)PdCl_2]^{2+}$ in gas phase

Table S25: Molecular orbital transition of the $RuPdCl_2$ complex in gas phase

States	**Transition**	**Orbital Transition**	**%**	**VEE (eV)**	**λ (nm)**	**f**
S1	278 → 279	d(Pd), n_{Cl} → π^*(tpphz)	90.1636	0.8658	1432.02	0.0000
S5	276 → 279	d(Pd), n_{Cl} → π^*(tpphz)	88.0783	1.2116	1023.31	0.0222
S37	276 → 286	d(Pd), n_{Cl} → π^*(tpphz)	64.5271	2.4611	503.78	0.0999
	278 → 288	d(Pd), n_{Cl} → π^*(bpy)	13.3851			
	278 → 289	d(Pd), n_{Cl} → π^*(tpphz)	13.8033			
S52	269 → 279	d(Ru), n_{Cl} → π^*(tpphz)	58.5340	2.7191	455.98	0.1580
	271 → 279	d(Ru), d(Pd), n_{Cl} → π^*(tpphz)	20.6995			
	273 → 283	d(Ru) → π^*(bpy),π^*(tpphz)	10.3176			
S67	269 → 282	d(Ru), n_{Cl} → π^*(tpphz)	12.8707	2.9596	418.92	0.1416
	269 → 283	d(Ru), n_{Cl} → π^*(bpy),π^*(tpphz)	26.9070			
	270 → 281	d(Ru) → π^*(bpy)	46.2568			
S74	270 → 282	d(Ru) → π^*(tpphz)	16.7574	3.0735	403.40	0.1127
	270 → 283	d(Ru) → π^*(bpy),π^*(tpphz)	66.0790			
S118	265 → 280	π(tpphz) → π^*(tpphz)	16.1028	3.7765	328.30	0.2506
	266 → 282	π(tpphz) → π^*(tpphz)	32.0560			
	266 → 283	π(tpphz) → π^*(bpy),π^*(tpphz)	42.0059			
S119	265 → 280	π(tpphz) → π^*(tpphz)	33.0972	3.8028	326.03	0.7067
	266 → 283	π(tpphz) → π^*(bpy),π^*(tpphz)	47.5469			
S206	261 → 283	π(bpy) → π^*(bpy),π^*(tpphz)	51.1708	4.5389	273.16	0.2899
	262 → 281	π(bpy) → π^*(bpy)	13.2180			
S210	261 → 281	π(bpy) → π^*(bpy)	29.0947	4.581	270.65	0.6416
	262 → 283	π(bpy) → π^*(bpy),π^*(tpphz)	33.0078			

S4.2 Acetonitrile

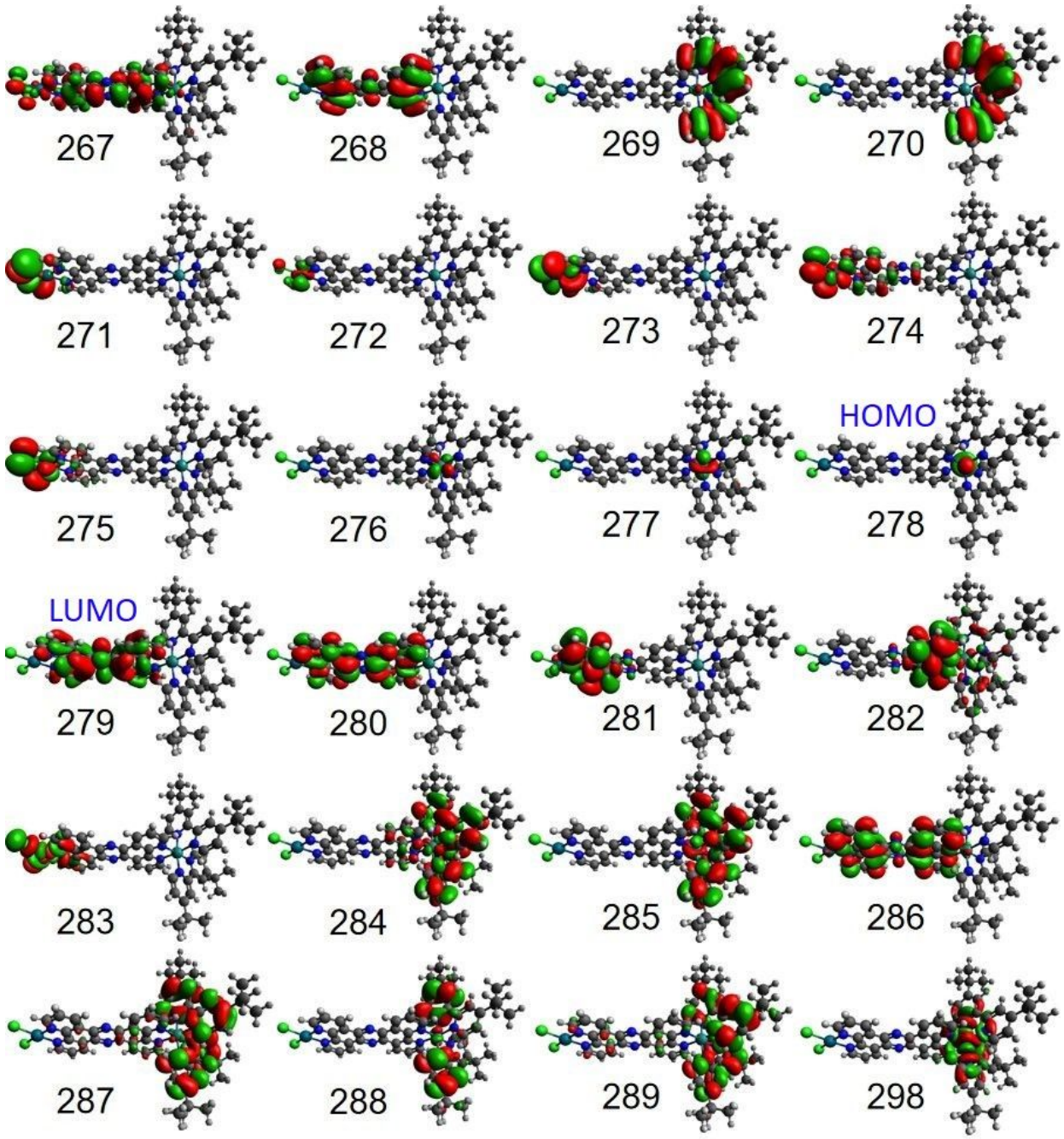

Figure S13: Frontier orbitals of $([(tbbpy)_2Ru(tpphz)PdCl_2]^{2+}$ in acetonitrile

Table S26: Molecular orbital transitions of the $RuPdCl_2$ complex in acetonitrile

States	**Transition**	**Orbital Transition**	**%**	**VEE (eV)**	**λ (nm)**	**f**
S1	278 → 279	d(Ru) → π^*(tpphz)	88.9671	2.1645	572.81	0.0004
S3	276 → 279	d(Ru) → π^*(tpphz)	95.9140	2.3472	528.22	0.0518
S12	276 → 282	d(Ru) → π^*(tpphz)	61.5096	2.7857	445.07	0.1513
	276 → 284	d(Ru) → π^*(bpy)	30.0592			
S16	276 → 282	d(Ru) → π^*(tpphz)	14.2087	2.8653	432.71	0.1672
	276 → 284	d(Ru) → π^*(bpy)	39.7636			
	277 → 285	d(Ru) → π^*(bpy)	38.9845			
S18	276 → 285	d(Ru) → π^*(bpy)	59.4966	2.9108	425.95	0.1514
	277 → 284	d(Ru) → π^*(bpy)	37.9390			
S24	274 → 279	d(Pd), n_{Cl} → π^*(tpphz)	92.6868	3.2078	386.51	0.1730
S40	277 → 286	d(Ru) → π^*(tpphz)	81.3017	3.6112	343.33	0.1077
S43	267 → 279	d(Pd), n_{Cl}, π(tpphz) → π^*(tpphz)	33.3973	3.6529	339.41	0.1693
	270 → 279	π(bpy) → π^*(tpphz)	31.7636			
	276 → 287	d(Ru) → π^*(bpy)	10.0074			
S56	276 → 288	d(Ru) → π^*(bpy)	78.4629	3.8723	320.18	0.1346
	278 → 289	d(Ru) → π^*(bpy)	14.5562			
S66	267 → 281	d(Pd), n_{Cl}, π(tpphz) → π^*(tpphz)	20.0028	4.0542	305.82	1.0275
	268 → 280	π(tpphz) → π^*(tpphz)	34.8362			
S73	268 → 280	π(tpphz) → π^*(tpphz)	15.2153	4.1301	300.20	0.3042
	270 → 282	π(bpy) → π^*(tpphz)	13.2407			
	278 → 298	d(Ru) → d*(Ru)	29.2551			
S98	269 → 285	π(bpy) → π^*(bpy)	74.2542	4.4502	278.60	0.2608
S101	269 → 284	π(bpy) → π^*(bpy)	27.4867	4.4797	276.77	0.9604
	270 → 285	π(bpy) → π^*(bpy)	43.6907			

S5 Orbital Transition of the $RuPtCl_2$ Photocatalyst

S5.1 Gas Phase

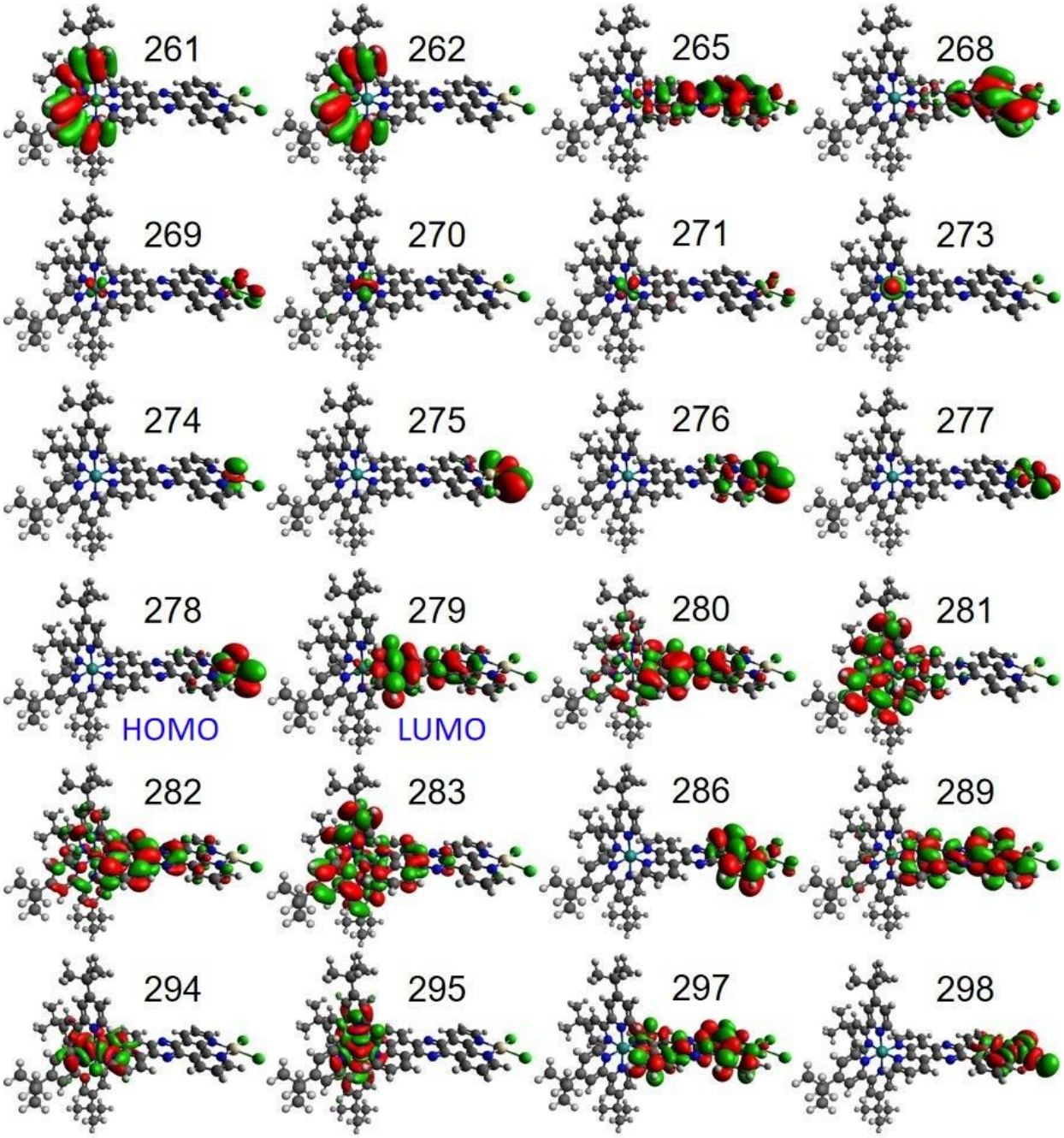

Figure S14: Frontier orbitals of $([(tbbpy)_2Ru(tpphz)PtCl_2]^{2+}$ in gas phase

Table S27: Molecular orbital transitions of the $RuPtCl_2$ complex in gas phase

States	**Transition**	**Orbital Transition**	**%**	**VEE (eV)**	**λ (nm)**	**f**
S1	278 → 279	d(Pt), n_{Cl} → π^*(tpphz)	89.1006	0.8027	1544.59	0.0001
S5	276 → 279	d(Pt), n_{Cl} → π^*(tpphz)	79.9682	1.1453	1082.55	0.0288
S39	276 → 286	d(Pt), n_{Cl} → n_{Cl}, π^*(tpphz)	71.3272	2.4904	497.85	0.1713
	278 → 289	d(Pt), n_{Cl} → π^*(tpphz)	25.1057			
S51	269 → 279	d(Ru), d(Pt), n_{Cl} → π^*(tpphz)	17.5635	2.7236	455.22	0.1441
	271 → 279	d(Ru), d(Pt), n_{Cl} → π^*(tpphz)	59.7893			
S62	270 → 281	d(Ru) → π^*(bpy)	45.6968	2.9581	419.13	0.1421
	271 → 282	d(Ru) → π^*(tpphz), π^*(bpy)	12.2206			
	271 → 283	d(Ru) → π^*(tpphz), π^*(bpy)	22.2151			
S102	265 → 279	d(Pt) → π^*(tpphz)	47.2042	3.658	338.94	0.224
	265 → 280	d(Pt) → π^*(tpphz)	22.9666			
	268 → 282	d(Pt) → π^*(tpphz), π^*(bpy)	19.2324			
S116	265 → 280	π(tpphz) → π^*(tpphz)	40.4118	3.8241	324.22	0.8144
	268 → 283	d(Pt) → π^*(tpphz), π^*(bpy)	17.4711			
	278 → 297	d(Pt), n_{Cl} → π^*(tpphz)	17.6834			
S195	261 → 283	π(bpy) → π^*(tpphz), π^*(bpy)	53.3586	4.5413	273.01	0.3577
	262 → 281	π(bpy) → π^*(bpy)	13.8928			
S201	261 → 281	π(bpy) → π^*(bpy)	27.1526	4.5836	270.50	0.5994
	262 → 283	π(bpy) → π^*(tpphz), π^*(bpy)	30.9039			

S5.2 Acetonitrile

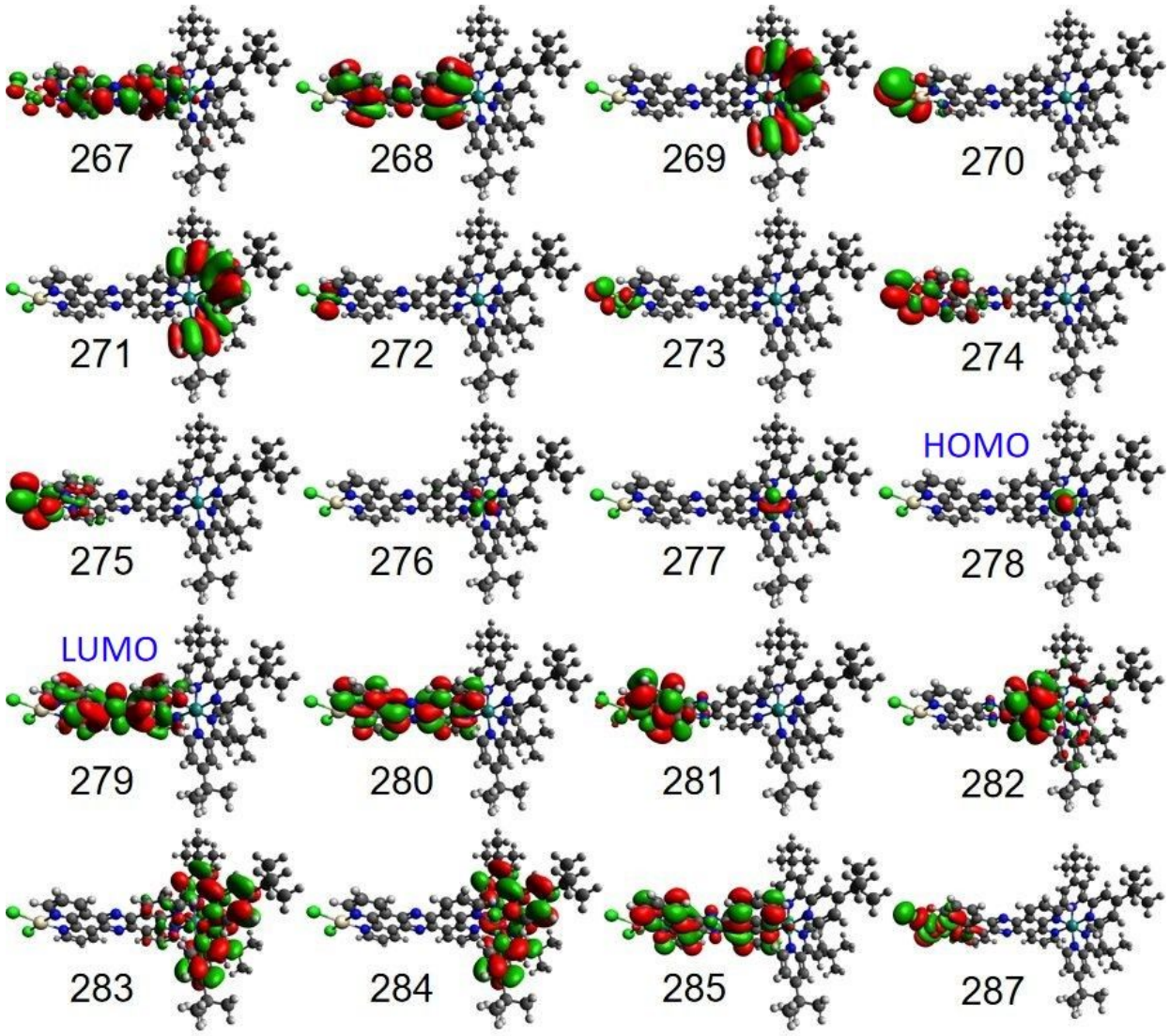

Figure S15: Frontier orbitals of $[(tbbpy)_2Ru(tpphz)PtCl_2]^{2+}$ in acetonitrile

Table S28: Molecular orbital transitions of the $RuPtCl_2$ complex in acetonitrile

States	**Transition**	**Orbital Transition**	**%**	**VEE (eV)**	**λ (nm)**	**f**
S1	278 → 279	d(Ru) → π^*(tpphz)	89.4400	2.1547	575.41	0.0005
S3	277 → 279	d(Ru) → π^*(tpphz)	95.8392	2.3366	530.62	0.0518
S11	276 → 282	d(Ru) → π^*(tpphz)	64.0825	2.7838	445.38	0.1695
	276 → 283	d(Ru) → π^*(bpy)	27.7647			
S15	276 → 282	d(Ru) → π^*(tpphz)	12.3604	2.8634	433.00	0.1729
	276 → 283	d(Ru) → π^*(bpy)	42.0646			
	277 → 284	d(Ru) → π^*(bpy)	38.1798			
S16	276 → 284	d(Ru) → π^*(bpy)	59.4050	2.9114	425.86	0.1522
	277 → 283	d(Ru) → π^*(bpy)	38.0890			
S38	267 → 279	d(Pt), n_{Cl} → π^*(tpphz)	42.6223	3.6404	340.58	0.2330
	271 → 279	π(bpy) → π^*(tpphz)	43.6683			
S65	267 → 281	d(Pt), n_{Cl} → π^*(tpphz)	13.6221	4.044	306.59	0.7409
	268 → 280	π(tpphz) → π^*(tpphz)	23.7898			
	274 → 283	d(Pt), n_{Cl} → π^*(bpy)	27.3460			
S100	269 → 283	π(bpy) → π^*(bpy)	27.8542	4.4794	276.79	0.9394
	271 → 284	π(bpy) → π^*(bpy)	43.6552			

References

(1) Sinstein, M.; Scheurer, C.; Matera, S.; Blum, V.; Reuter, K.; Oberhofer, H. Efficient Implicit Solvation Method for Full Potential DFT. *J. Chem. Theory Comput.* **2017**, *13*, 5582–5603.

(2) Fattebert, J.-L.; Gygi, F. Density functional theory for efficient ab initio molecular dynamics simulations in solution. *J. Comput. Chem.* **2002**, *23*, 662–666.

(3) Andreussi, O.; Dabo, I.; Marzari, N. Revised self-consistent continuum solvation in electronic-structure calculations. *J. Chem. Phys.* **2012**, *136*, 064102.

(4) Kirkwood, J. G. Theory of Solutions of Molecules Containing Widely Separated Charges with Special Application to Zwitterions. *J. Chem. Phys.* **1934**, *2*, 351–361.

(5) Hille, C.; Ringe, S.; Deimel, M.; Kunkel, C.; Acree, W. E.; Reuter, K.; Oberhofer, H.

Generalized molecular solvation in non-aqueous solutions by a single parameter implicit solvation scheme. *J. Chem. Phys.* **2019**, *150*, 041710.

(6) Marenich, A. V.; Cramer, C. J.; Truhlar, D. G. Universal Solvation Model Based on Solute Electron Density and on a Continuum Model of the Solvent Defined by the Bulk Dielectric Constant and Atomic Surface Tensions. *J. Phys. Chem. B* **2009**, *113*, 6378–6396.